Fabrication of All-Polymeric Photonic Bandgap Bragg Fibers Using Rolling of Coextruded PS/PMMA Multilayer Films

Stoeffler, Karen; Dubois, Charles; Ajji, Abdellah; Guo, Ning; Boismenu, Francis; Skorobogatiy, Maksim

Publisher's version / Version de l'éditeur:
https://doi.org/10.1002/pen.21631
Polymer Engineering and Science, 50, 6, 2009-12-23

Fabrication of All-Polymeric Photonic Bandgap Bragg Fibers Using Rolling of Coextruded PS/PMMA Multilayer Films

Karen Stoeffler,[1] Charles Dubois,[1] Abdellah Ajji,[2] Ning Guo,[3] Francis Boismenu,[3] Maksim Skorobogatiy[3]
[1] *École Polytechnique de Montréal, Génie Chimique, Montréal, Québec*

[2] *Institut des Matériaux Industriels, CNRC, Boucherville, Québec*

[3] *École Polytechnique de Montréal, Génie Physique, Montréal, Québec*

Photonic bandgap Bragg fibers feature periodic sequence of layers of different materials. In those particular waveguides, the wave path is controlled by a periodical spatial modification of the refractive index. Depending on the periodicity of the structure and on the refractive index contrast, a specific wavelength range is propagated along the fiber axis. In this work, we developed all-polymeric photonic bandgap Bragg fibers based on polystyrene (PS)/polymethyl methacrylate (PMMA) alternating layers. We describe a novel and efficient method for the preparation of the fibers preforms, and we present the fibers drawing process and the transmission properties of the resulting Bragg fibers. POLYM. ENG. SCI., 50:1122–1127, 2010. © 2009 Society of Plastics Engineers

INTRODUCTION

Polymeric photonic crystals waveguides have recently attracted considerable interest. Compared with conventional glass waveguides, polymeric materials offer several advantages: low cost, low processing temperatures, possibility of combining different materials, and of modifying the original materials (functionalization, incorporation of specific fillers, etc.). Polymeric photonic crystals waveguides have been recently used in various applications, including data communication [1–3], nonlinear optics [4], light amplification [5], sensors [6–8], THz guiding [9, 10], and biocompatible fibers for in vivo light delivery and sensing [11, 12].

Photonic crystal waveguides operate using a different guidance principle than total internal reflection (TIR), which is the basic guidance principle of conventional glass waveguides. In a photonic crystal, the wave path is controlled by a periodical spatial modification of the refractive index. The repetitive pattern forces the wave to scatter and interfere in a way that restricts its propagation only to certain directions and at certain frequencies [13]. Photonic crystals can be 1D, 2D, or 3D. Bragg fibers are based on 1D photonic crystals, which simply consist of multilayer films. The transmission intensity through a planar multilayer film depends on the periodicity of the stack and on its refractive index contrast. Some frequencies are strongly reflected and have almost no transmission through the stack (Fig. 1a, [13]): this range of frequency is called a photonic bandgap. If the multilayer film is rolled into a tube, the frequencies comprised into the photonic bandgap of the multilayer structure will be confined to the fiber core and will propagate along its length (Fig. 1b, [13]): this is the basic principle of wave propagation in multilayer Bragg fibers. Moreover, the core of multilayer Bragg fibers can be of low-refractive index material, or it can even be hollow. This is in strike contrast to the standard TIR waveguides that require for their operation a high-refractive index core surrounded by a lower refractive index cladding. Bragg fibers have recently been suggested for use in color changing and color-tunable textiles [14], for illumination and distributed sensing applications, for ultrasensitive sensors of the analyte refractive index [15], for applications in bio- and chemical sensors, as well as for high-bandwidth short-range telecommunication applications [3].

Bragg fibers can be fabricated by drawing macroscopic preforms in a draw tour to decrease the preform diameter by a factor of 50 to 100 (Fig. 2). Recently, our collaboration has developed two methodologies for fabricating multilayer Bragg fiber preforms [16]. The first approach uses deposition of alternating layers of two different polymers on the inside of a rotating polymer cladding tube by solvent evaporation. Using this method, polystyrene

Correspondence to: K. Stoeffler; e-mail: karen.stoeffler@polymtl.ca
DOI 10.1002/pen.21631
Published online in Wiley InterScience (www.interscience.wiley.com).

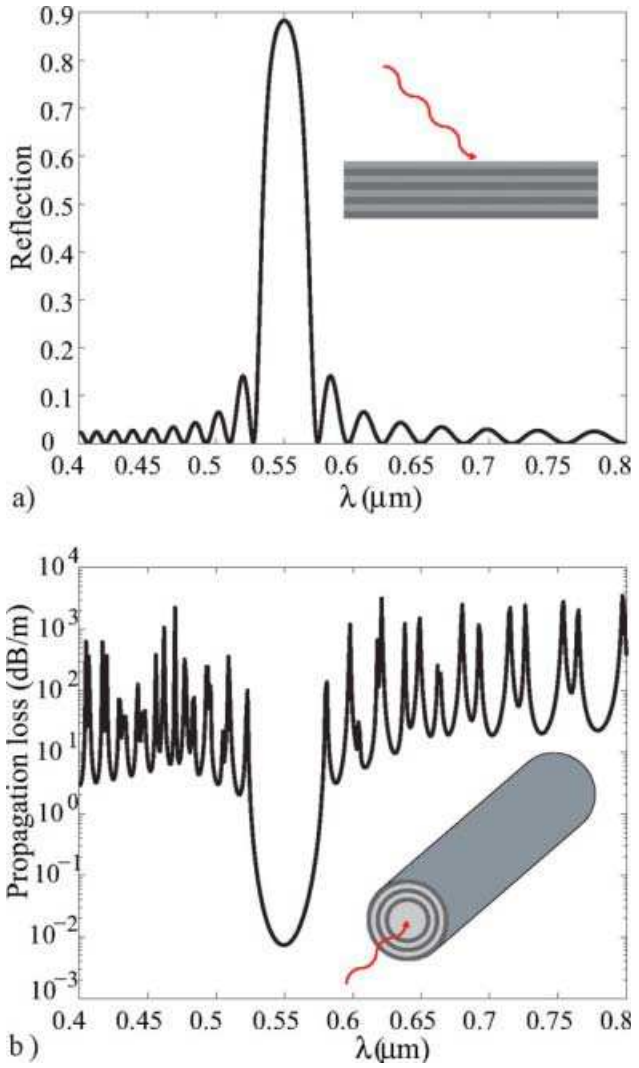

FIG. 1. Wave propagation through a multilayer film and through a photonic bandgap Bragg fiber. (a) For a multilayer film, there exists a frequency region called a photonic bandgap so that for a given angle of incidence onto the multilayer film, the light is efficiently reflected. For the frequencies inside the bandgap, the transmission through the multilayer reflector is effectively zero. (b) When the multilayer film is rolled into a cylindrical reflector around a solid or a hollow core, for the frequencies within the photonic bandgap, the light is strongly confined in the fiber core through consecutive reflections from the multilayer reflector. Thus, for the frequencies within the bandgap of the multilayer reflector, fiber transmission loss will be small. [Color figure can be viewed in the online issue, which is available at www.interscience.wiley.com.]

(PS)/polymethyl methacrylate (PMMA) and polycarbonate (PC)/polyvinylidene fluoride (PVDF) combinations were successfully obtained. This method has two major drawbacks. The first one is the necessity of finding two orthogonal solvents that do not cross solve the polymer during the periodically alternated deposition process. The second drawback is the time consuming step of solvent extraction from the resulting multilayer preforms. An alternative approach for multilayer preforms fabrication is a so-called corolling method that consists of rolling two different polymer films around a plastic rod or a plastic tube called mandrel. The mandrel can either be left as a part of a preform, thus forming a solid core, or it can be later removed for the fabrication of hollow core fibers. Although corolling method results in a spiral rather than a cylindrical structure, numerical simulations show that optical performances of the resulting fibers are virtually identical. The corolling method allows fabrication of preforms containing ~100 layers arranged in a periodic sequence. Major disadvantage of the corolling method, however, is its highly mechanical nature. Trapping of air microbubbles inside the multilayer structure is particularly challenging to avoid. Such defects strongly affect the optical loss of the resulting fibers. This phenomenon is still aggravated when the microvoids are located within the first few layers closest to the fiber core. In this article, we present a novel method for preparing multilayer preforms, based on the modified corolling method. We aim at suppressing the formation of microvoids within the multilayer structure. This is achieved by rolling a single multilayer film around a mandrel rather than corolling two monolayer films. In what follows, we describe the PS/PMMA multilayer film extrusion, rolling of the multilayer preform, drawing of the multilayer Bragg fiber, and finally, characterization of the multilayer Bragg fiber transmission properties.

MATERIALS

The materials used for the fabrication of the multilayer Bragg fibers are polystyrene (PS, Polystyrene 535, Total Petrochemicals; MFI = 4 g/10 min, 200°C/5 kg; ρ = 1040 kg/m^3) and polymethyl methacrylate (PMMA, Plexiglas V825, Altuglas International, Arkema; MFI = 3.7 g/10 min, 230°C/3.8 kg; ρ = 1190 kg/m^3). In the visible regime, the refractive indices of those materials are, respectively, 1.59 and 1.49 [17].

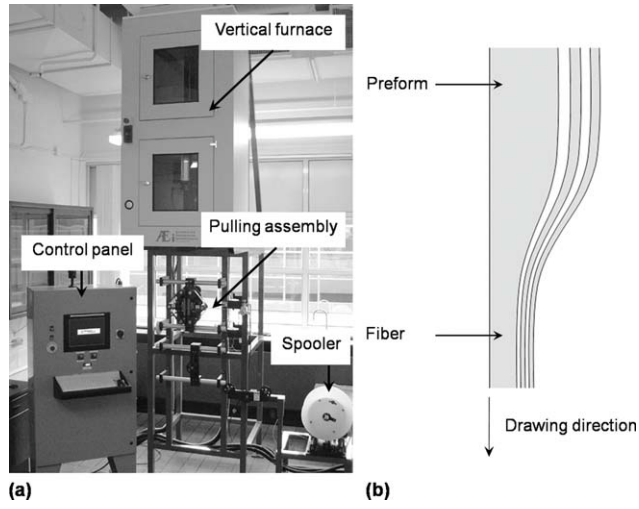

FIG. 2. Schematic of the fiber drawing process. (a) Photograph of the draw tower; and (b) Schematic of the neck-down region during drawing of a Bragg fiber.

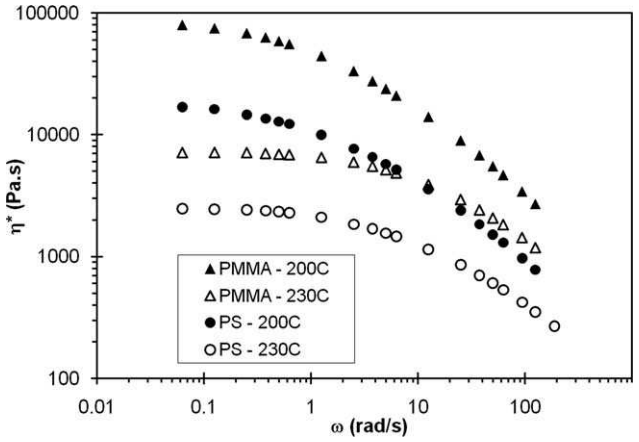

FIG. 3. Rheological behavior of PS and PMMA at 200°C and 230°C.

Those polymer grades were mainly selected as a function of their melt flow index, since the various materials constituting the multilayer Bragg fiber must have comparable rheological properties at the extrusion and drawing temperatures. The rheological behavior of both materials was investigated through small amplitude oscillatory rheometry using a stress controlled rheometer (CSM, Bohlin) in a nitrogen environment. The geometry consisted of a 25-mm parallel plate configuration. Tests were carried out at 230°C (extrusion temperature) and at 200°C (drawing temperature). Samples were thermally stabilized in the rheometer for a period of 600 s before testing. The region of linear viscoelastic behavior was determined using stress sweeps experiments. A constant stress of 300 Pa was chosen for both materials to conduct the linear viscoelastic measurements. Time sweeps experiments performed at 1 Hz and 300 Pa did not show any significant degradation on a time period of 1 h for PS. For PMMA, the variation $\Delta\eta^*$ of complex viscosity was +9%, which was considered acceptable. Thus, frequency sweeps were performed between 0.01 and 30 Hz under a constant stress of 300 Pa (Fig. 3). As expected from the melt flow index values, PMMA is slightly more viscous than PS. At low shear rates comparable to the ones experienced during the drawing process, the viscosities of PMMA and PS are, respectively, 8×10^4 Pa s and 2×10^4 Pa s. This could affect the deformation of the adjacent layers during the drawing process. However, those viscosity values remain in the same order of magnitude.

MULTILAYER FILM EXTRUSION AND CHARACTERIZATION

Four-layer PS/PMMA film (overall thickness: 80 μm) was coextruded using two twin screw extruders (extruder A: Coperion Werner & Pfleiderer ZSK-40, $D = 40$ mm, $L/D = 40$; extruder B: Coperion Werner & Pfleiderer ZSK-25 WLE, $D = 25$ mm; $L/D = 40$) and one single screw extruder (extruder D: Killion KTS-100, $D = 1\ 1/4''$, $L/D = 24$). Before extrusion, PMMA was dried for 4 h at 82°C. Both PS and PMMA were extruded at 230°C. The extrusion configuration was ADBD. PMMA was fed to extruders A and B, whereas PS was fed to extruder D.

From the consideration of optical performance optimization [18], thicknesses of the individual layers in the multilayer zone of a Bragg fiber have to be comparable to the wavelength of light transmitted through such fibers. Thus, for applications in the visible spectral range, individual layer thicknesses in the multilayer reflector should be comparable to 500 nm. As multilayer reflector of the fiber is drawn from the rolled multilayer film in the preform, the thickness of the individual layers in the preform can be determined by multiplying the desired layer thickness in the fiber by the drawdown ratio used during the drawing process. A typical drawdown ratio used in our experiments is 50; thus, defining the thickness of the individual layers in the preform to be in the order of 25 μm.

To achieve such layer thicknesses in the extruded film, flow rates of 8 kg/h were gravimetrically controlled for extruders A and B (PMMA), whereas the flow rate of extruder D (PS) was approximately set to ~13 kg/h. The overall volumetric repartition of PS and PMMA in the resulting four-layer film was verified by means of spectroscopic measurements using a Varian Cary 5000 UV–Vis-NIR spectrophotometer operating between 1300 and 2900 nm. Particularly, PS and PMMA have specific absorption peaks, respectively, located at 2477 and 2253 nm (Fig. 4). The intensity of those specific peaks was measured as a function of the film thickness in the range of 25 to 100 μm for the pure materials (Fig. 5). From this calibration, the volumetric ratio of PS to PMMA in the four-layer film was found to be 1.04. Microtomed cross sections of the extruded four-layer film were observed using a scanning electron microscope (SEM) Hitachi S4700 operating under a 2 kV voltage. The repartition of the various layers was uniform within the film width. The respective thick-

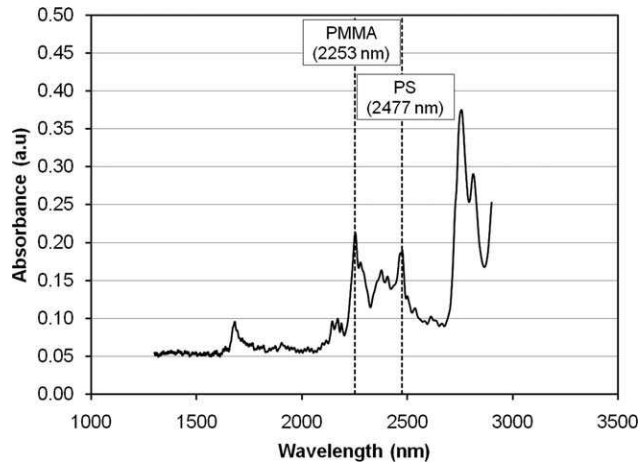

FIG. 4. Absorption spectrum of a four-layer coextruded PS/PMMA film of total thickness 80 μm.

 DOI 10.1002/pen

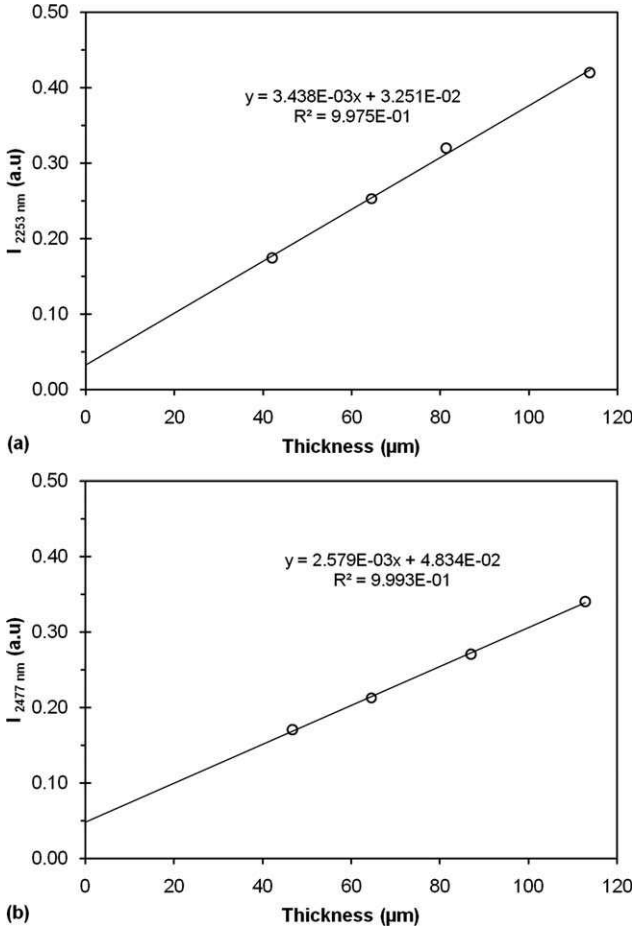

FIG. 5. Calibration curves of absorbance as a function of the material thickness: (a) PMMA and (b) PS.

nesses of the PS and PMMA layers were found to be ~22 μm and ~18 μm (Fig. 6).

MULTILAYER BRAGG FIBER PREPARATION AND CHARACTERIZATION

To produce a solid core Bragg fiber, the four-layer PS/PMMA film was rolled around a PMMA rod (diameter: 12 mm; length: 30 cm), which was annealed at 90°C for 48 h in a vacuum oven before use. The rolled preform was then placed tightly into a 3-mm thick and 30-cm long PMMA cladding tube, as shown on Fig. 7a. The preform was mounted in the draw tower and was consolidated at 140°C for 4 h before being drawn at 200°C. In view of varying the spectral position of the photonic bandgap, various drawing velocities were used to obtain fibers with external diameters ranging from 300 to 500 μm.

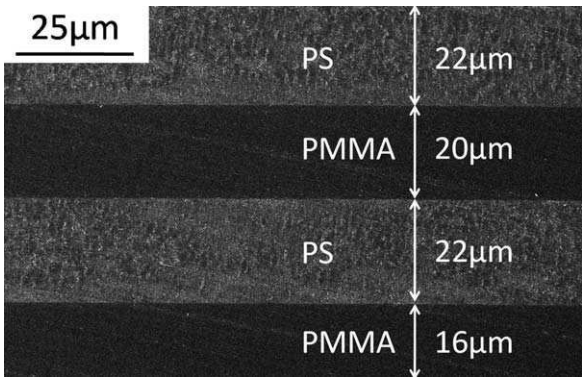

FIG. 6. Four-layer coextruded PS/PMMA film observed by FEG-SEM.

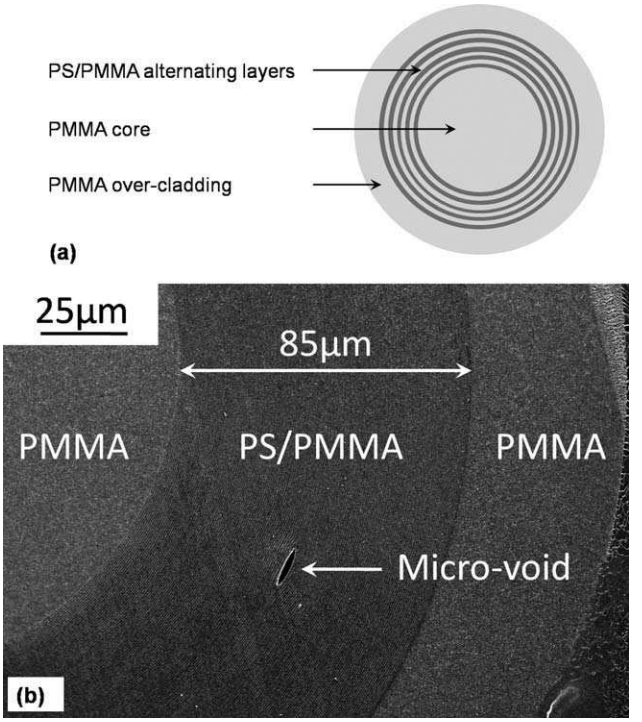

FIG. 7. (a) Schematic of the cross section of a Bragg fiber, and (b) micrograph of a Bragg fiber of the 500 μm external diameter.

Micrographs of a Bragg fiber of external diameter 500 μm are shown on Figs. 7 and 8. FEG-SEM microscopy reveals that the overall thickness of the ~150 layers reflector in the Bragg fiber is ~85 μm (Fig. 7b). The individual layers have a uniform thickness of ~550 nm (Fig. 8b), meaning that the viscosity mismatch is not significant enough to affect the drawing process. Figures 7b and 8a also reveal the presence of a microvoid, probably created during the preparation of the preform. However, this defect is not located within the first alternating layers, and consequently, it is not supposed to affect the optical properties of the fiber.

OPTICAL PROPERTIES

Transmission through the Bragg fibers was studied using a super continuum white-light source focused by an objective into the fiber core center. The fiber transmission spectra were recorded with the aid of a monochromator. A typical fiber length studied in the transmission experiment was ~50 cm. Upon launching white light, all the spectral components not guided by the reflector bandgap

were irradiated in the first 1–3 cm along the fiber length. Subsequently, only a specific color guided by the bandgap was propagated to the fiber [11]. Figure 9 shows the transmission spectra of the Bragg fibers in the visible region as a function of their diameter. The transmission range is 475 to 625 nm (green to yellow) for fibers of diameter 400 μm, and 500 to 725 nm (yellow to red) for fibers of diameter 500 μm. This result confirms that the transmission properties of the Bragg fibers can be easily modified by controlling the overall drawing ratio, and thereby the thickness of the alternating PS/PMMA layers.

CONCLUSIONS

In this work, solid core Bragg fibers composed of ~150 PS/PMMA alternating layers were produced according to new process in which a four-layer PS/PMMA extruded film was rolled around a PMMA rod to make a preform that was subsequently drawn into a fiber. Compared with the alternative processes based on the deposition of alternating layers by solvent casting, or by corolling of monolayer PS and PMMA films, this new method presents the following advantages: (i) the number of defects, especially in the optically important first few layers, is greatly reduced; (ii) the thickness and uniformity of the individual layers can be easily controlled; (iii) a high number of alternating layers can easily be reached; and (iv) the preparation of the preform is less time consuming. The resulting Bragg fibers were demonstrated to guide specific wavelengths in the visible range depending on their diameter.

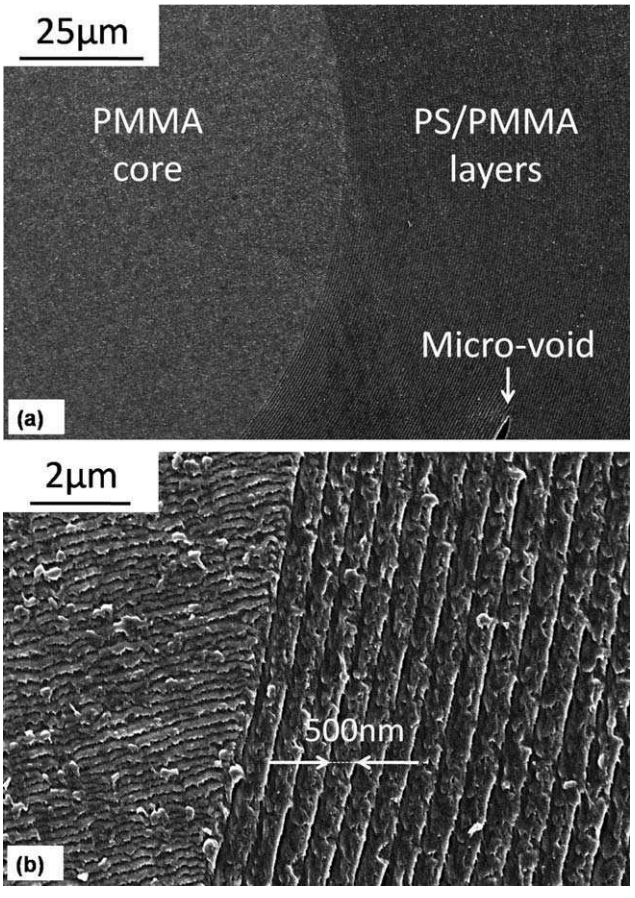

FIG. 8. FEG-SEM details of a Bragg fiber of external diameter 500 μm: (a) low magnification and (b) first 15 alternating layers at high magnification.

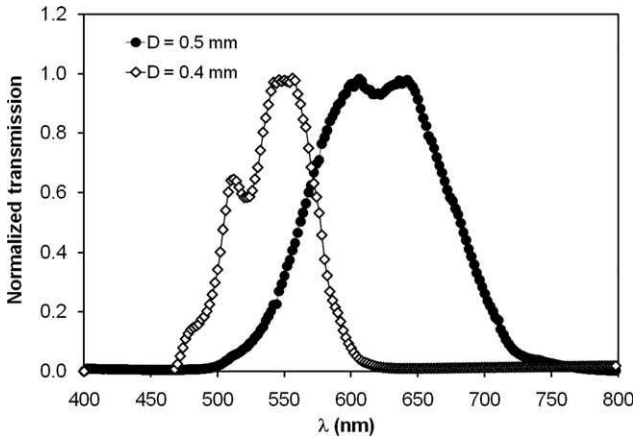

FIG. 9. Transmission spectra of two PS/PMMA Bragg fibers of different diameters.

ACKNOWLEDGMENTS

The authors are grateful to Total Petrochemicals and Arkema who kindly donated the polymeric materials used for this project.

REFERENCES

1. Y. Koike, T. Ishigure, and E. Nihei, *J. Lightwave Technol.*, **13**, 1475 (1995).
2. M.A. van Eijkelenborg, A. Argyros, A. Bachmann, G. Barton, M.C.J. Large, G. Henry, N.A. Issa, K.F. Klein, H. Poisel, W. Pok, L. Poladian, S. Manos, and J. Zagari, *Electron. Lett.*, **40**, 592 (2004).
3. M. Skorobogatiy and N. Guo, *Opt. Lett.*, **32**, 900 (2007).
4. D.W. Garvey, K. Zimmerman, P. Young, J. Tostenrude, J.S. Townsend, Z. Zhou, M. Lobel, M. Dayton, R. Wittorf, M.G. Kuzyk, J. Sounick, and C.W. Dirk, *J. Opt. Soc. Am. B*, **13**, 2017 (1996).
5. K. Kuriki, Y. Koike, and Y. Okamoto, *Chem. Rev.*, **102**, 2347 (2002).
6. C.M.B. Cordeiro, M.A.R. Franco, G. Chesini, E.C.S. Barretto, R. Lwin, C.H. Brito Cruz, and M.C.J. Large, *Opt. Express*, **14**, 13056 (2006).
7. A. Argyros, M.A. van Eijkelenborg, M.C.J. Large, and I.M. Bassett, *Opt. Lett.*, **31**, 172 (2006).
8. A. Hassani and M. Skorobogatiy, *J. Opt. Soc. Am. B*, **24**, 1423 (2007).
9. H. Han, H. Park, M. Cho, and J. Kim, *Appl. Phys. Lett.*, **80**, 2634 (2002).
10. M. Skorobogatiy and A. Dupuis, *Appl. Phys. Lett.*, **90**, 113514 (2007).

 DOI 10.1002/pen

11. A. Dupuis, N. Guo, Y. Gao, N. Godbout, S. Lacroix, C. Dubois, and M. Skorobogatiy, *Opt. Lett.*, **32**, 109 (2007).
12. G. Emiliyanov, J.B. Jensen, O. Bang, A. Bjarklev, P.E. Hoiby, L.H. Pedersen, E. Kjaer, and L. Lindvold, *Opt. Lett.*, **32**, 460 (2007).
13. M. Skorobogatiy and J. Yang, *Fundamentals of Photonic Crystal Guiding*, Cambridge University Press, New York (2009).
14. B. Gauvreau, N. Guo, K. Schicker, K. Stoeffler, F. Boismenu, A. Ajji, R. Wingfield, C. Dubois, and M. Skorobogatiy, *Opt. Express*, **16**, 15677 (2008).
15. M. Skorobogatiy, "Resonant Bio-Chemical Sensors Based on Photonic Bandgap Waveguides and Fibers," in *Optical Guided-Wave Chemical and Biosensors*, M. Zourob and A. Lakhtakia, Eds., Springer Series on Chemical Sensors and Biosensors, Springer-Verlag, New York (2009).
16. Y. Gao, N. Guo, B. Gauvreau, M. Rajabian, O. Skorobogata, E. Pone, O. Zabeida, L. Martinu, C. Dubois, and M. Skorobogatiy, *J. Mater. Res.*, **21**, 2246 (2006).
17. J. Brandrup, E.H. Immergut, E.A. Grulke, A. Abe, and D.R. Bloch, *Polymer Handbook*, *4th ed.*, Wiley, New York (2005).
18. M. Skorobogatiy, *Opt. Lett.*, **30**, 2991 (2005).